

Frustration in The Coupled Rattler System $\text{KO}_{\text{Os}_2\text{O}_6}$

J. Kuneš^{1,2} and W.E. Pickett¹

¹*Department of Physics, University of California, Davis CA 95616, USA**

²*Institute of Physics, Academy of Sciences of the Czech Republic,
Cukrovarnická 10, 162 53 Praha 6, Czech Republic*

(Dated: June 22, 2018)

PACS numbers: 74.70.Dd,63.20.Pw,63.70.+h

The phenomenon of frustration, which gives rise to many fascinating phenomena, is conventionally associated with the topology of non-bipartite lattices, where nearest-neighbor (nn) interactions and global connectivity compete in the lowering of energy. The issue of rattling atoms in spacious lattice sites is a separate occurrence that can also lead to a high density of low energy states (unusual low temperature thermodynamics) and to practical applications such as in improved thermoelectric materials. In this letter we address a unique situation where both phenomena arise: a four-fold single-site instability leads to rattling of cations on a diamond structure sublattice where nn interactions frustrate simple ordering of the displacements. The system deals with this coupling of rattling+frustration by commensurate ordering. Such a disorder-order transition may account for the second phase transition seen in $\text{KO}_{\text{Os}_2\text{O}_6}$ within the superconducting state, and the unusual low-energy dynamics and associated electron-phonon coupling can account for the qualitative differences in physical properties of $\text{KO}_{\text{Os}_2\text{O}_6}$ compared to RbOs_2O_6 and CsOs_2O_6 , all of which have essentially identical average crystal and electronic structures.

The pyrochlore-lattice-based structure with a potential to support magnetic frustration has attracted attention to $\text{AO}_{\text{Os}_2\text{O}_6}$ ($\text{A}=\text{K, Rb, Cs}$) group. Unexpectedly large variation of the superconducting T_c throughout the group (from 3.3 K in CsOs_2O_6 to 9.7 K in $\text{KO}_{\text{Os}_2\text{O}_6}$) [1, 2, 3] together with reports of anomalous nuclear spin relaxation [4] and indications of anisotropic order parameter [5] in $\text{KO}_{\text{Os}_2\text{O}_6}$ pointed to a possibility of unconventional pairing and fueled the early experimental interest. While the issue of superconductivity remains controversial in the light of recent pressure experiments [1], unusual transport and thermodynamic properties were found in the normal state of $\text{KO}_{\text{Os}_2\text{O}_6}$ in sharp contrast to the standard metallic behavior of RbOs_2O_6 and CsOs_2O_6 [6, 7, 8].

Uniquely to $\text{KO}_{\text{Os}_2\text{O}_6}$ within this class, the normal-state conductivity exhibits a non-Fermi-liquid behavior characterized by a concave temperature dependency down to low temperatures [9, 10]. The low temperature linear specific heat coefficient is estimated to be substantially

larger than in RbOs_2O_6 and CsOs_2O_6 [10]. Recently an intriguing λ -shaped peak in the specific heat was observed in good quality $\text{KO}_{\text{Os}_2\text{O}_6}$ single-crystals indicative of a phase transition at $T_p = 7$ K [10], within the superconducting state. This observation was recently confirmed [9]. Notably, the peak position and shape do not change even when the superconductivity is suppressed below 7 K by the external field. Insensitivity to such a profound change of the electronic state indicates that the peak is rooted in the lattice dynamics rather than intrinsic electronic degrees of freedom.

Electronic structure investigations [11, 12] have revealed a considerable bandwidth of the $\text{Os-5d-}t_{2g}$ 12-band complex of about 3 eV which does not support the idea of local moment formation on the Os sites nor any emergence of frustration due to the pyrochlore topology of the Os sublattice, made of a three-dimensional network of vertex-sharing tetrahedra. Instead we find that a significant frustration, not magnetic but structural, takes place on the diamond sublattice occupied by K ions. We have shown previously [11] that the symmetric (A_g) potassium phonon mode is unstable and that the energy can be lowered by several meV/atom(K) through rather large displacements of the K ions. Here we construct, based on first principles calculations, the effective potential describing fourfold symmetric displacements of K ions off their ideal diamond-lattice sites, with nn coupling leading to a highly frustrated system of displacements. Dynamical simulations for finite clusters reveal a classical ground state with complex pattern of displacements.

In Fig. 1 we show the $\text{AO}_{\text{Os}_2\text{O}_6}$ lattice which consists of Os on a pyrochlore sublattice, having one O atom bridging each Os nn pair. The cavities in the Os-O network are filled with alkali ions, which themselves form a diamond lattice, composed of two *fcc* sublattices. Using a full-potential linearized augmented-plane-waves code Wien2k [13] we have performed a series of calculations in which K ions move along the (111) direction: (i) the two *fcc* sublattices are displaced in opposite direction (symmetric A_g mode), (ii) same as (i) with the O positions allowed to relax, (iii) only one *fcc* sublattice is displaced. Comparing results (i) and (ii) reveals a non-negligible O relaxation only for large K displacement ξ_i (the energy vs displacement curve has slightly less steep walls when O ions are allowed to relax). Since the O re-

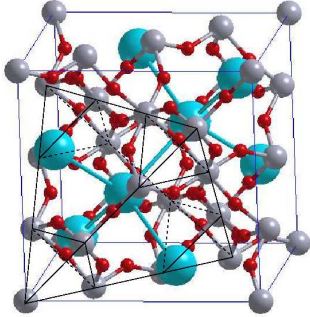


FIG. 1: **The AOs₂O₆ lattice.** The atomic species are maker with different colors: Os (gray), O (red) and alkali metal (blue). The pyrochlore sublattice of Os atoms is highlighted. Notice the alkali sublattice with diamond structure.

laxation effect is minor we consider the Os-O network to be rigid for the following discussion. The inter-ionic distances together with the geometry of the Os-O network with spacious channels along the nn K-K bonds suggest nn coupling to dominate over longer range interaction. The effective Hamiltonian becomes

$$\hat{H} = \sum_i \left[\frac{p_i^2}{2M} + P_e(\xi_i) + P_o(\xi_i) \mathcal{Y}_{32}(\hat{\xi}_i) \right] + \sum_{i>j} W_{ij}(\xi_i, \xi_j), \quad (1)$$

where the first term is the on-site Hamiltonian and second describes the nn coupling (interaction). The on-site potential, which captures the essential tetrahedral local symmetry, consists of a spherical and the next non-zero term in spherical harmonic expansion (\mathcal{Y}_{lm}), while the radial dependency is described by even and odd 6th-order polynomials $P_e(\xi_i)$ and $P_o(\xi_i)$ obtained by fitting the *ab initio* data from type (iii) calculations (Fig. 2).

We have solved the quantum-mechanical single site problem by numerical integration on real space grid (details of the calculation can be found in Ref. 14). The low energy spectrum up to 80 K (containing 20 states) is characterized by a singlet-triplet split ground state (8 K splitting) separated by a gap of about 25 K from excited states. This essential difference from the harmonic potential with singlet ground state is reflected also by a Schottkyesque anomaly in the single-site specific heat.[14] The sharpness of the observed peak, however, rules out the Schottky anomaly scenario, pointing instead to a collective transformation involving inter-site coupling. A particularly useful way of looking at the quasi-degenerate quadruplet ground state, is in terms of four symmetry related local orbitals centered in the local minima. A

weak coupling of about -2 K for each pair of orbitals accounts for the singlet-triplet splitting.

Ab initio calculations [11] revealed much less anharmonicity in the Rb and especially Cs potentials, which can treated as a perturbation and neglected for the present purposes. Within this approximation Rb (Cs) dynamics is described by 3D oscillator with a frequency of 44 K (61 K). Recent analysis of specific heat data by Brühwiler *et al.* [9] led to a frequency of 60 K for RbOs₂O₆, which we find a reasonable agreement given the approximations. Localized modes were previously observed in specific heat of RbOs₂O₆ and CsOs₂O₆ by Hiroi *et al.*[15] The harmonic oscillator root mean square displacement is

$$\Delta = \sqrt{\langle \xi_i^\alpha)^2 \rangle} = \frac{1}{\sqrt{2M\omega}}, \quad \alpha = x, y, z, \quad (2)$$

and we obtain $\Delta_{Rb} = 0.15a_0$ (Bohr radius) and $\Delta_{Cs} = 0.1a_0$ for the mean square displacement at zero temperature, which we will use below in estimation of strength of the inter-site coupling.

The interaction can be obtained by following the force acting on a fixed ion when its neighbors are uniformly displaced. The simplest form of central pair force that describes reasonably well the *ab initio* data is $F(\mathbf{r}) = A\frac{\mathbf{r}}{r} + B\mathbf{r}$, corresponding to a pair potential $V(\mathbf{r}_1, \mathbf{r}_2) = A|\mathbf{r}_{12}| + \frac{B}{2}|\mathbf{r}_{12}|^2$ (\mathbf{r}_j are ion coordinates). In Fig. 2(inset) we show the first principles force together with the model fit, the values $A=-88$ mRy/a₀ and $B=7.9$ mRy/a₀² are essentially the same for all three oxides. As expected from its electrostatic origin the pair force is repulsive for admissible values of r . Using the electrostatic force $-\frac{1}{r^2}$ instead of an *ad hoc* Taylor expansion, the force in Fig. 2 would not crossover to the positive values, but only reach zero for zero displacement. The observed behavior is qualitatively consistent with faster decay of the interaction due to screening. The interaction $W_{ij}(\xi_i, \xi_j)$ between ions at sites \mathbf{R}_i and \mathbf{R}_j is obtained after subtraction of contributions accounted for in the on-site potential:

$$W_{ij}(\xi_i, \xi_j) = V(\mathbf{R}_i + \xi_i, \mathbf{R}_j + \xi_j) - V(\mathbf{R}_i, \mathbf{R}_j + \xi_j) - V(\mathbf{R}_i + \xi_i, \mathbf{R}_j) + V(\mathbf{R}_i, \mathbf{R}_j). \quad (3)$$

The result is a directional (non-central) potential, whose dipolar form becomes clear in the small displacement limit:

$$\tilde{W}_{ij}(\xi_i, \xi_j) \approx A \frac{(\mathbf{R}_{ij} \cdot \xi_i)(\mathbf{R}_{ij} \cdot \xi_j)}{R_{ij}^3} - \left(\frac{A}{R_{ij}} + B \right) \xi_i \cdot \xi_j. \quad (4)$$

We start the discussion of nn coupling in the simpler quasiharmonic case (RbOs₂O₆ and CsOs₂O₆). Small mean displacements justify the use of a dipolar approximation (4) to estimate the interaction energy. Using the Schwarz inequality $|\langle \xi_i \cdot \xi_j \rangle|^2 \leq \langle \xi_i^2 \rangle \langle \xi_j^2 \rangle$ the interaction

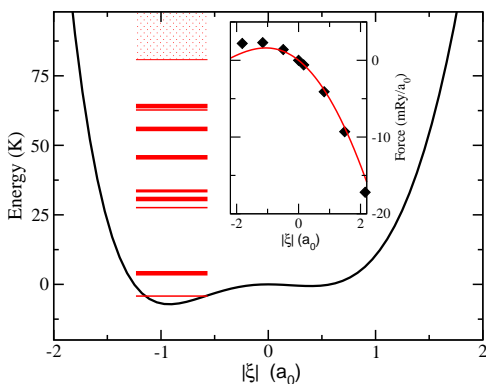


FIG. 2: **The on-site potential.** The on-site potential along the nn bond direction (the nn site is in the direction of positive x-axis). The vertical line denote the eigenenergies on the same scale, the thickness represents degeneracy ranging from 1 to 3. In the inset force acting on undisplaced ion as a function of the uniform displacement of its neighbors is shown. The symbol represent the *ab initio* data, the full line is the fit with linear pair force.

energy per site for a two-site problem has the following upper bound

$$|\langle \tilde{W} \rangle| \leq \left(\frac{|B|}{2} + \frac{|A|}{R} + B \right) \Delta^2, \quad (5)$$

yielding 23 K and 10 K for Rb and Cs respectively. Going one step further and considering the problem of four sites connected to their common neighbor the upper bound is reduced for purely geometrical reasons to 16 K and 7 K respectively. Smallness of the interaction energy in comparison to the Einstein frequencies and the singlet character of the on-site groundstate lead to conclusion that Rb and Cs dynamics is essentially local.

KOs₂O₆ presents the *opposite limit* of extreme anharmonicity, leading to quasi-degeneracy of the ground state and large spatial fluctuations, together with important inter-site coupling. In the following we evaluate the matrix elements of W in the basis of products $|\alpha\rangle$ of the on-site eigenstates. The basis of local orbitals for the ground state quadruplet has an advantage of keeping the Hamiltonian in quasi-diagonal form by maximizing the diagonal terms $\langle \alpha\beta | W | \beta\alpha \rangle$ and minimizing the leading off-diagonal contributions $\langle \alpha\beta | W | \gamma\alpha \rangle$. Moreover there is a natural one-to-one mapping between the local orbitals and nn bonds, namely we denote an orbital and a bond with the same index if the orbital represents displacement in the direction of the bond. Due to the symmetry there are only four independent diagonal matrix elements, which can be expressed in the form (in kelvins):

$$\begin{aligned} \langle \alpha\beta | W_R | \beta\alpha \rangle = & -324\delta_{\alpha\beta} + 742\delta_{\alpha R}\delta_{\beta R} \\ & -301(\delta_{\alpha R} + \delta_{\beta R}) + 147, \end{aligned} \quad (6)$$

where both the bond index R and the orbital indices α , β run from 1 to 4. These numbers can be understood in terms of the approximate formula (4), taking into account the inversion symmetry about the bond center. The relevant off-diagonal terms yield about 15 K (additional 2 K comes from the on-site Hamiltonian). The off-diagonal terms also provide coupling to products including excited states with the largest ones being about 1/3 of the corresponding energy difference, providing thus small but non-negligible quantum mechanical coupling.

Origin of frustration. Building a lattice model from bonds (6) helps to understand frustrated nature of the present system. Although it is not justifiable to neglect the excited states completely, they will only renormalize the parameters without changing the form of the four-state form of the Hamiltonian in the low energy sector. Building a lattice Hamiltonian from the bonds (6), using the fact that the third term yields a constant when summed over the bonds, we get an expression

$$H = \sum_{ij} (a\delta_{\alpha\beta}^{ij} + b^\infty \delta_{\alpha R(ij)}^i \delta_{\beta R(ij)}^j) + H_{\text{on-site}}. \quad (7)$$

The first term of (7) is the classical Potts Hamiltonian [16], $\delta_{\alpha\beta}^{ij}$ yields 1 when the neighboring sites i , j are occupied by the same state and zero otherwise. In the second term $R(ij)$ is an index of the bond between sites i and j , $\delta_{\alpha R(ij)}^i$ yields 1 if orbital on site i corresponds to displacement in the direction of the bond ij and zero otherwise. The bare values of parameters a and b are -162 K and 371 K respectively. Since the second term describes states whose energy is above the already neglected excited states it is consistent to rule these states out by putting b equal to $+\infty$. The second term thus becomes a constraint on admissible configurations and introduces frustration into the system. The leading quantum mechanical correction $H_{\text{on-site}}$, bare value of which is an order of magnitude smaller than a , is provided by tunneling between the local orbitals. Filling the lattice such that we minimize the contribution of an arbitrary first site (only 3 bonds can yield a due to the constraint) one can readily see that an arrangement with the same energy cannot be placed on the neighboring sites. Unlike in the case of geometrical frustration of nn antiferromagnets no odd-length loops are necessary to produce frustration. In fact the above mechanism would apply even to Bethe lattice with no loops at all. While we cannot make conclusions about the degeneracy of the groundstate, the frustrating constraint is expected to reduce the transition temperature below the energy scale defined by parameter a .

Dynamical simulations. While the effective Hamiltonian (7) can be useful for investigating general features

of the phase transition and is well suited for analytical approach, in the rest of this paper we pursue a separate, purely numerical approach to probe aspects of the ordering that we anticipate at T_p . Addressing this question in full generality is very difficult. Insight can be gained by minimizing the potential energy, i.e. pursuing the classical (large mass M) limit, for finite clusters with periodic boundary conditions. This is still a formidable computational task due to a large number of local minima. To approach and possibly reach the global minimum we have used a damped molecular dynamics combined with simulated annealing. In particular we have integrated the classical equation of motion

$$M \frac{d^2\boldsymbol{\xi}}{dt^2} = \mathcal{F}(\boldsymbol{\xi}) - \beta(T) \frac{d\boldsymbol{\xi}}{dt} + \mathcal{G}(T) \quad (8)$$

where \mathcal{F} is the actual force, the $\beta(T) \propto \sqrt{T}$ is a friction parameter and $\mathcal{G}(T)$ is a Gaussian random vector with half-width proportional to T . The effective temperature T was successively reduced, $T_i = \epsilon T_{i-1}$ ($\epsilon < 1$), until minimum was reached.

The minimum of the $1 \times 1 \times 1$ (single primitive cell) cluster can be described as parallel displacement of all ions along one of the bond directions with different displacement values ($1.54a_0$ toward the nn site and $1.24a_0$ away from nn site) on the two sublattices (the global minimum is of course degenerate with respect to the sublattice exchange). The ordering on a $2 \times 2 \times 2$ cluster is characterized by uniform displacements along different bonds as shown in Fig. 3. The minima for $3 \times 3 \times 3$ and larger clusters are difficult to understand in real space since the displacements are neither uniform nor limited to bond directions. Nevertheless, common features include a small net displacement per sublattice (less than $0.1a_0$) and an average displacement of $2.0a_0$ per site with a standard deviation of about $0.3a_0$. The size of displacements is likely to be overestimated due to neglect of the kinetic energy, effect of which can be qualitatively visualized as replacing the point particles with probability density clouds. Moreover Fourier transform of the displacement vectors $\xi_\alpha(\mathbf{R}_i)$

$$S_\alpha(\mathbf{q}) = \frac{1}{N} \sum_i \exp(i\mathbf{q} \cdot \mathbf{R}_i) \xi_\alpha(\mathbf{R}_i), \quad (9)$$

revealed that there are only a few non-vanishing \mathbf{q} -components for each cluster size. Even with the lowest cooling rate we were not able to obtain the minimum for $5 \times 5 \times 5$ cluster unambiguously, which strongly suggests that periodicity of 5 unit cells is not commensurate with the ordering tendencies in the system. The results are summarized in Table I. Fourier transforms are characterized by 2 or 3 dominant components with $(2/3, 2/3, 0)$ and $(1/2, 1/2, 1/2)$ appearing whenever allowed by the cluster size. Comparison of the minimum energies for different clusters indicates that beyond $3 \times 3 \times 3$ the energetics

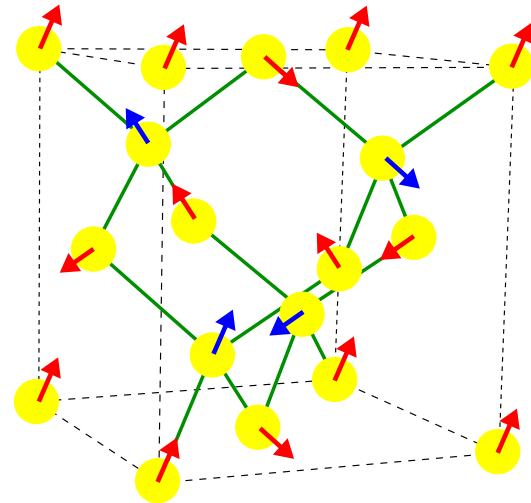


FIG. 3: Minimum energy configuration for $2 \times 2 \times 2$ cluster. Different colors correspond to the two fcc sublattices, green lines mark the nn bonds. (Note that the same displacements for sites on the same edge of the cube are not enforced by the boundary conditions.)

becomes very flat while the ordering wavevectors are sensitive to boundary conditions. The absolute value of this energy has no relevance for low energy scale of the ordering transition, but its convergence indicates that minimum energy is being reached.

Our results provide a picture of potassium dynamics in KOs_2O_6 governed by an effective Hamiltonian characterized by an unusually soft and broad local potential, which allows for large excursions of K ions resulting in significant and frustrating nn coupling. To address the question of ordering tendencies we have used classical simulations for finite clusters which provide a complicated but distinct pattern with multiple- \mathbf{q} ordering and large displacements. Since the purely numerical model is not well suited for addressing general questions concerning the phase transition and for understanding the essence of the present physics we have also proposed an analytic model with only a few parameters. This model is formally a three-dimensional ferromagnetic four-state Potts model with an additional constraint on possible configurations. While the unconstrained model is known

TABLE I: Minimum potential energy and the dominant Fourier components (only one member of $\pm\mathbf{q}$ pair is shown) for the ground states of clusters of different size (in brackets). The vectors are in the units of $\frac{2\pi}{a}$ where $a=10.101 \text{ \AA}$.

cluster size	E (mRy)	largest $ S(\mathbf{q}) $ for
$1 \times 1 \times 1$ (2)	-1.99	
$2 \times 2 \times 2$ (16)	-17.11	$(1,0,0), (0,1,0), (0,0,1)$
$3 \times 3 \times 3$ (54)	-18.01	$(-\frac{2}{3}, 0, \frac{2}{3}), (\frac{2}{3}, 0, \frac{2}{3})$
$4 \times 4 \times 4$ (128)	-18.11	$(\frac{1}{2}, \frac{1}{2}, -\frac{1}{2}), (-\frac{1}{4}, \frac{1}{4}, \frac{3}{4}), (\frac{1}{4}, \frac{3}{4}, \frac{1}{4})$
$6 \times 6 \times 6$ (432)	-18.20	$(0, -\frac{2}{3}, \frac{2}{3}), (-\frac{2}{3}, \frac{1}{2}, \frac{1}{2}), (\frac{2}{3}, \frac{1}{6}, \frac{5}{6})$

to exhibit a first order mean-field-like phase transition [16], the constraint cannot be relieved in a simple way by the system and is likely to change behavior of the model.

Our calculations suggest a natural explanation for the second peak observed in the specific heat of $\text{KO}_{\text{S}_2}\text{O}_6$ [10] as a phase transition of the potassium sublattice to supercell order. Anomalies of low temperature electronic properties such as non-Fermi-liquid conductivity and large linear specific heat coefficient [10] can be explained as consequence of atomic motion, which does not freeze down to the ordering transition at 7 K. We point out that large excursions of K ion should affect the NMR measurements due to quadrupolar interaction and might be responsible for observed anomalies [4]. The dynamics of Rb and Cs ions is very different: the local behavior is quite different due to the larger ionic radii which gives a different energy scale, and this distinction in turn negates the inter-site interaction, leaving a simple quasiharmonic local mode. This result of our first principle calculations fits well with the observed specific heat and conductivity [9, 15].

If it proves possible, synthesis of $\text{K}_x\text{Rb}_{1-x}\text{Os}_2\text{O}_6$ will provide a means of introducing ‘vacancies’ into the model Hamiltonian (7). The combination of rattling and frustrating nn interaction, facilitated by ‘fine tuning’ of the potassium ionic radius to the size of osmium-oxygen cage, provides a novel physical system, which exhibits a phase transition as low temperature.

We acknowledge discussions with R. R. P. Singh and R. Seshadri, and communication with Z. Hiroi, M. Brühwiler, and B. Batlogg. J.K. was supported by DOE grant FG02-04ER 46111 and Grant No. A1010214 of Academy of Sciences of the Czech Republic, and W.E.P was supported by National Science Foundation grant No. DMR-0421810.

- [2] S. Yonezawa *et al.*, New Pyrochlore Oxide Superconductor RbOs_2O_6 , *J. Phys. Soc. Japan* **73**, 819-821 (2004) see also [17].
- [3] S. Yonezawa, Y. Muraoka, and Z. Hiroi, New β -Pyrochlore Oxide Superconductor CsOs_2O_6 , *J. Phys. Soc. Japan* **73**, 1655-1656 (2004).
- [4] K. Arai *et al.*, 39K and 87Rb Nuclear Magnetic Resonance in the Pyrochlore Superconductors $\text{AO}_{\text{S}_2}\text{O}_6$ (A=K, Rb), *cond-mat/0411460*
- [5] A. Koda *et al.*, Possible Anisotropic Order Parameter in Pyrochlore Superconductor $\text{KO}_{\text{S}_2}\text{O}_6$ Probed by Muon Spin Rotation, *J. Phys. Soc. Japan* **74**, 1678-1681 (2005).
- [6] R. Khasanov *et al.*, Pressure Effects on the Transition Temperature and the Magnetic Field Penetration Depth in the Pyrochlore Superconductor RbOs_2O_6 , *Phys. Rev. Lett.* **93**, 157004 (2004).
- [7] T. Schneider, R. Khasanov, and H. Keller, Evidence for Charged Critical Behavior in the Pyrochlore Superconductor RbOs_2O_6 , *Phys. Rev. Lett.* **94**, 077002 (2005).
- [8] K. Magishi *et al.*, Evidence for s-wave superconductivity in the β -pyrochlore oxide RbOs_2O_6 , *Phys. Rev. B* **71**, 024524 (2005).
- [9] M. Brühwiler private communication.
- [10] Z. Hiroi *et al.*, Second Anomaly in the Specific Heat of beta-Pyrochlore Oxide Superconductor $\text{KO}_{\text{S}_2}\text{O}_6$, *J. Phys. Soc. Japan*, **74** 1682-1685 (2005) see also [17].
- [11] J. Kuneš, T. Jeong, and W. E. Pickett, Correlation effects and structural dynamics in the β -pyrochlore superconductor $\text{KO}_{\text{S}_2}\text{O}_6$, *Phys. Rev. B* **70**, 174510 (2004).
- [12] R. Saniz *et al.*, Electronic structure properties and BCS superconductivity in -pyrochlore oxides: $\text{KO}_{\text{S}_2}\text{O}_6$, *Phys. Rev. B* **70** 100505(R) (2004).
- [13] P. Blaha *et al.*, Wien2k, *An Augmented Plane Wave + Local Orbitals Program for Calculating Crystal Properties* (Karlheinz Schwarz, Techn. Universität Wien, Wien, 2001), ISBN 3-9501031-1-2.
- [14] J. Kuneš and W. E. Pickett, $\text{KO}_{\text{S}_2}\text{O}_6$: superconducting rattler, to appear in *Physica B*.
- [15] Z. Hiroi *et al.*, Specific Heat of the β -Pyrochlore Superconductors CsOs_2O_6 and RbOs_2O_6 , *J. Phys. Soc. Japan* **74**, 1255-1262 (2005) see also [17].
- [16] F. Y. Wu, The Potts model, *Rev. Mod. Phys.* **54**, 235-268 (1982).
- [17] Z. Hiroi *et al.*, Erratum to Three Papers on β -Pyrochlore Oxide Superconductors, *J. Phys. Soc. Japan* **74**, 3400 (2005).

* Electronic address: jkunes@physics.ucdavis.edu

[1] T. Muramatsu *et al.*, Anomalous Pressure Dependence of the Superconducting Transition Temperature of β -Pyrochlore Oxides $\text{AO}_{\text{S}_2}\text{O}_6$, *Phys. Rev. Lett.* **95**, 167004 (2005).